Journal of Engineering and Sustainable Development
https://jeasd.uomustansiriyah.edu.iq/index.php/jeasd
https://doi.org/10.31272/jeasd.27.6.7

Vol. 27, No. 06, November 2023
ISSN 2520-0917

Original Research

OPTIMAL LONG-RANGE-WIDE-AREA-NETWORK PARAMETERS CONFIGURATION FOR INTERNET OF VEHICLES APPLICATIONS IN SUBURBAN ENVIRONMENTS

Gregor A. Aramice[1*], Abbas H. Miry[2], Tariq M. Salman[3]

Electrical Engineering Department, College of Engineering, Mustansiriyah University, Baghdad, Iraq
[1]https://orcid.org/0000-0003-0990-5781
[2]https://orcid.org/0000-0002-7456-287x
[3]https://orcid.org/0000-0003-1614-8627

Received 12/02/2023 ***Revised 22/03/2023*** ***Accepted 12/04/2023***

Abstract: In this paper, the effect of Long-Range wireless technology parameters on signal propagation in suburban environments is investigated. Wireless propagation modeling provides information about the wireless channel and its impact on communication links. Received signal strength and coverage area are evaluated to determine signal path loss. The operating frequency of 433 MHz Long Range Wireless Area Network is utilized with different spreading factors, bandwidths, and code rates. Empirical propagation models are utilized to predict a mathematical model based on measured empirical signal strength in a suburban site in Baghdad City. The measured signal strength and signal-to-noise ratio values were obtained through drive tests in an Internet of Vehicles environment to design a network that could accurately report vehicle locations. The LoRa parameters affected the calculated path loss exponent, leading to various predictions in the network design. The path loss exponent exhibited instability due to the presence of obstacles and different long-range parameter settings. Path loss exponent deviation fluctuates due to bandwidth and spreading factor variations. Path loss exponent reduced at higher coding rates for more protection purposes. Packet ratio reception improved as the coding rate increased. To minimize the impact of the path loss on network design, an optimization policy was employed to determine the best parameters that resulted in the lowest path loss. The optimal path loss obtained at LoRa configuration parameters settings with spreading factor (7), bandwidth (500 kHz), and code rate (4/5).

Keywords: *Path-loss model prediction; path-loss exponent; Internet-of-Things; Vehicle-to-Infrastructure; Vehicular-Ad-Hoc-Networks*

1. Introduction

The Internet of Things (IoT) is a network system in which various devices and applications are interconnected through the Internet. This includes devices such as phones, computers, home appliances, vehicles, and many other electronic devices. Each device or application has its unique identification and can communicate with other devices on the network [1]. A special case of IoT is the Internet of Vehicles (IoV), shown in Fig. 1, which refers to the integration of Internet connectivity into vehicles, allowing them to communicate with other vehicles, infrastructure, and devices. This technology can enhance safety, improve traffic flow, and provide drivers with new services and information. It also enables the development of autonomous vehicles, as well as smart cities and transportation systems. Examples of IoV applications include vehicle-to-vehicle

*Corresponding Author:
gregoralexander1977@uomustansiriyah.edu.iq

communication for collision avoidance, traffic congestion warning, and real-time traffic information [2].

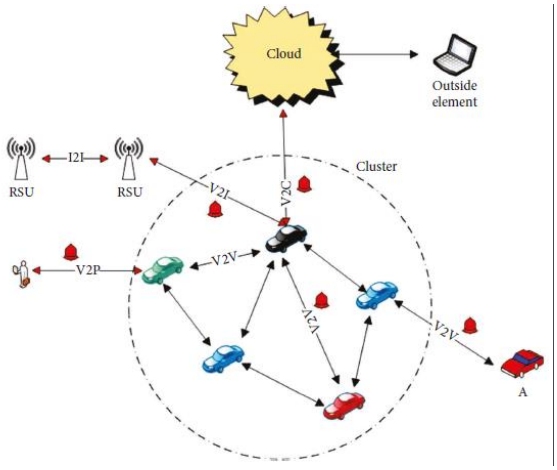

Figure 1. IoV communications [2].

One of the network architectures to perform IoV communication is the Long Range Wide Area Network (LoRaWAN) based Long Range (LoRa) modulation technology [3]. LoRa is the physical layer of LoRaWAN, it developed by Semtech Corporation [4].

Many researchers discussed the indoor design of LoRaWAN and produced its performance and link quality.

Designing a wireless network requires determining the maximum distance between nodes that still guarantees a dependable wireless connection [5]. Many technical parameters may play a role in a wireless network design such as transmitter (TX) power, operating frequency, and receiver (RX) sensitivity [6]. In LoRa the configuring parameters may affect the LoRaWAN communication quality and propagation links, such parameters are Spreading Factor (SF), Bandwidth (BW), and Code Rate (CR).

Path Loss (PL) models play a crucial role in wireless communication, predicting the performance of the transmission link between TX and RX in channels. These models aid in the planning and design of wireless networks [7].

The design of LoRaWAN depends on the PL calculation through predicting the propagation models, since these models assist radio engineers in improving the performance of communication networks through design and optimization [8].

This paper focuses on the outdoor environment to study the performance and link quality of the LoRaWAN at 433MHz frequency in IoT applications, especially IoV applications with Vehicle-to-Infrastructure (V2I) communication. Some of the contributions of this paper are to measure the Received Signal Strength (RSS), and analyzing the performance in terms of tuning the LoRa module parameters to analyze packet loss and Signal-to-Noise Ratio (SNR) between LoRaWAN TX and RX.

2. Related Works

Several studies examined the relationship between TX and RX performance in various environments and settings, using a range of wireless communication technologies, through the use of propagation modeling. Identifying an accurate propagation model for propagation losses is a significant concern that can aid in providing the most precise PL prediction when designing wireless communication networks [9]. LoRa technology is one of these wireless technologies which utilized as a basis of LoRaWAN design for IoT applications. LoRa configuration parameters are set according to the application it is utilized for. LoRa configuration parameters affect PL estimation due to the effect of these parameters on the PL modeling in which an empirical measurement depends on the Path Loss Exponent (PLE).

Hence, LoRa parameters affect the link (performance and quality) due to the selected combinations of parameter configurations. The following works related to PL modeling utilizing different propagation models based LoRa technology at different operating frequencies and various environments.

In Karttunen et al.'s study [10], an urban area was studied at 28GHz operating frequency to extract a weighted fitting distance-dependent PL propagation model. In Allen et al.'s study [11], a mix of outdoor-indoor PL models was extracted at different operating frequencies utilizing Singular Value Decomposition (SVD) with Least Mean Square (LMS) Error. In Unterhuber et al.'s study [12], different PL propagation models were studied at 5.2GHz for Train-to-Train (T2T) communication PL modeling for monitoring purposes via information exchange to get precise location and speed of trains in rural, suburban, and tunnel areas. In Bertoldo et al.'s study [13], indoor propagation assessment indicated that Keenan's model is the best model to be used for an office radio link design based LoRa with an operating frequency 868MHz. In Ingabire et al.'s study [14], outdoor propagation investigation was performed on four propagation models with an operating frequency 868MHz in an urban IoT environment with LoRaWAN technology. Two estimation results were obtained, COST-231 Hata and Okumura Hata models both underestimate the RSS while Extended Hata and ITU R 1225 models both over-estimate the RSS. In Zakaria et al.'s research [15], two areas were studied (urban and suburban) for PL propagation modeling at 3.5GHz operating frequency with two PLEs extracted for each area. PLE is environment dependent and it varies from 2 to 4 [16].

The following works are related to PL evaluation-based LoRa parameter configurations set at different operating frequencies, various environments, and analyzing methods.

In Wu et al., Callebaut et al., and Lin et al.'s studies [17-19], PL evaluation of LoRa link in an outdoor environment at operating frequencies 433MHz and 868MHz at transmitting powers 0dBm, 13dBm, and 20dBm respectively were studied to get maximum PL that limited with LoRa RX sensitivity according to the derived PL model. In Callebaut et al.'s study [18], PL evaluation was performed of point-to-point LoRa connections using low-height terminals. A higher PL is encountered, resulting in more lost packets due to the lower RSS, in comparison to a typical star topology network that has a base station at a higher elevation. In Kongsavat et al.'s study [7], smart meter-based LoRaWAN technology was designed at 920-925MHz operating frequencies with 12dBm transmitting power proposing PL model in urban areas utilizing Root Mean Square Error (RMSE) for evaluating and comparing the proposed model with standard propagation models. The obtained result is that the predicted model error is less than Okumura-Hata model. In Lin et al.'s study [20], after modeling an underground LoRa-based wireless channel, it was found that increasing BW leads to reduced sensitivity which leads to a degradation in receiving signal quality since the data rate increased due to BW increasing. On the contrary, when increasing SF, the data rate decreases with an improvement in link quality, an increase in communication reliability and propagation distance. In Akram et al.'s study [21], Time on Air (ToA) was studied according to SF and BW parameters variation. ToA increased as SF increased, and it reduced when BW increased. In Anzum et al.'s study

[22], the propagation of LoRa technology was studied through empirical measurements taken at a frequency of 433 MHz in a palm oil plantation. The LoS measurements were utilized to determine the PLE, with the SFs revealing distinct propagation characteristics, resulting in a significant change in the PLE. The PLE varies depending on the BW and SF. It was discovered that an increase in BW leads to a decrease in both the communication range and sensitivity.

3. Long Range Technology

The LoRa wireless communication technology is utilized for transmitting data over ranges of kilometers 5Km–15Km, adopts Chirp Spread Spectrum modulation with SF ranging from 7 to 12 and data rate between 30bps to 50Kbps [23, 24]. Additionally, to long-range coverage, this technology stands on some properties which are: high robustness, multipath resistance, very high immunity to Doppler Effect, and low power consumption. LoRa transceivers may operate in Industrial, Scientific, and Medical (ISM) frequency bands 868MHz and 433MHz (EU), 915MHz and 433MHz (USA) [25].

Different protocols (star, mesh) can utilize LoRa. LoRaWAN Media Access Control (MAC) defines communication protocols and systems with three classes (A, B, and C) [26]. Fig. 2 depicts LoRaWAN architecture, which consists of End Nodes, Gateways (GWs) or base stations, and Servers, establishing Node-to-Server communication through the GWs provided with an (IP) [27].

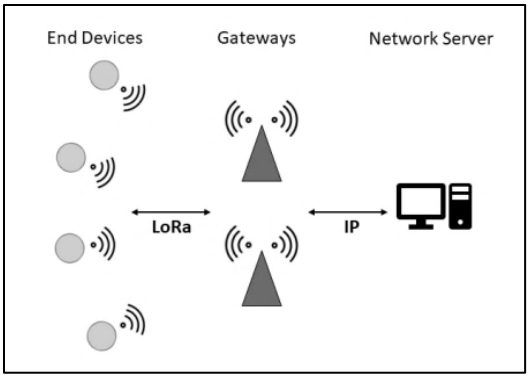

Figure 2. LoRaWAN architecture [28].

4. Semtech SX1278 LoRa Module

The Semtech SX1278, shown in Fig. 3, is a long-range, low-power wireless transceiver module that utilizes the LoRa modulation technology [29]. The Semtech SX1278 LoRa module is capable of measuring the RSS Indicator (RSSI) and SNR of incoming radio signals [20].

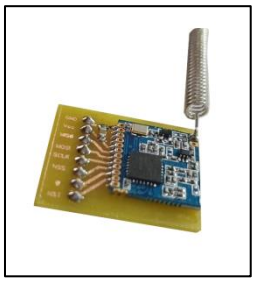

Figure 3. Semtech SX1278 LoRa Module [30].

5. LoRa Configuration Parameters

The effectiveness of LoRa is affected by physical factors: SF, BW, and CR. These parameters impact bit rate and LoRa noise resistance. But in general, five configuration parameters were selected in LoRa radio to determine communication link performance when designing LoRaWAN at suburban sites, these tunable parameters are Transmission Power (TP), Carrier Frequency (CR), SF, BW, and CR. Briefed elucidations of these parameters are:

Transmission Power: LoRa module has adjustable TP from (-4 to 20) dBm with steps of unity dB. This range was selected to be from (2 to 20) dBm due to implementation restrictions [1]. Increasing TP extends signal range but this leads to shortened battery life [31].

Carrier Frequency: It represents the center frequency of the transmission BW [32]. For the Semtech SX1278 chip, the range of CF may be adjusted from (137 to 525) MHz [29].

Spreading Factor: It is the ratio between the symbol rate and the chip rate. For Semtech SX1278, SF ranges from (6 to 12) in unity steps, each SF represents an orthogonal separated channel and may be used for transmission in LoRaWAN network separately without affecting each other [1]. The amount 2^{SF} represents the number of chips per symbol, and it increases as SF increases. Any increase in SF increases packet transmission duration, SNR, distance and RX sensitivity but data rate decreases, which means slow transfer of information [31]. SF may be selectable or adaptable since depending on the distance between TX and RX the end terminals in LoRaWAN tend to use higher SFs to fix the weak signal reception but for strong signals, these terminals tend to use lower SF, and this done on the cost of information transmission speed [32]. The SF controls the number of chirps and by increasing it, the range can be expanded [18].

Bandwidth: It is the transmission band range of frequencies. For Semtech SX1278 the allowed programmable values are (10.4, 15.6, 20.8, 31.25, 41.7, 62.5, 125, 250, and 500) kHz. As BW increases data rate increases but both ToA and sensitivity decrease [31].

Code Rate: It is LoRa Forward Error Correction (FEC) rate for bursts of interference protection to provide robust communication links. The allowable CRs with LoRa are (4/5, 4/6, 4/7 and 4/8). Increasing CR provides much protection but with an increase in ToA. LoRa TXs/RXs with different CRs and fixed (SF, BW, and CF) make communication links still available [31, 32].

In this paper, Semtech SX1278 transceiver module was utilized for both transmitting and receiving, with parameter limits shown in Table 1, with the selected values in this work which provide 24 possible configuration combinations, as explained in Table 2.

Table 1. Semtech SX1278 module (allowed limits and selected values) configuration parameters

Configuration Parameters	Allowed Limits	Selected Values
TP	2 to 17 dBm	17 dBm
CF	137 to 525 MHz	433MHz
BW	10.4, 15.6, 20.8, 31.25, 41.7, 62.5, 125, 250 and 500 kHz	125, 250 and 500 kHz
SF	6 to 12	7, 9, 10 and 12
CR	1 to 4 (Cyclic CR=4/CR+4)	1 for 4/5 and 3 for 4/7

Table 2. The Selected Parameters Configuration Combinations

BW \ SF	7	9	10	12
125 kHz	CR= 4/5, 4/7	CR= 4/5, 4/7	CR= 4/5, 4/7	CR= 4/5, 4/7
250 kHz	CR= 4/5, 4/7	CR= 4/5, 4/7	CR= 4/5, 4/7	CR= 4/5, 4/7
500 kHz	CR= 4/5, 4/7	CR= 4/5, 4/7	CR= 4/5, 4/7	CR= 4/5, 4/7

6. Path Loss Models

Properties of a radio communication channel include the operating frequency, the antennas used, and the nature of the propagation environment. To analyze a communication channel, it is necessary to consider radio signal propagation [33]. PL models are used to anticipate a decline in signal power or RSS and these models vary depending on the environment such as free space, suburban, and urban. Factors such as the nature of the environment, the distance between TX and RX, and the heights of the TX and RX antennas, also affect PL [19].

The free space model in Eq. (1) is used to describe the reduction in the (RSS) at the Line of Site (LoS) path [34]:

$$P_L(d) = 20\log_{10} d + 20\log_{10} f + 20\log_{10}(\frac{4\pi}{c}) \quad (1)$$

Where $P_L(d)$ is the PL at distance (d) which is the distance separating TX and RX, (f) is the operating frequency, and (c) is the speed of light.

The log-distance PL model is the most commonly utilized PL model for suburban and urban areas. The log-distance PL model is described in terms of distance (d) and PLE (γ) and expressed as Eq. (2) [35]:

$$P_L(d) = P_L(d_0) + 10\gamma\log_{10}\left({}^{d}/_{d_0}\right) \quad (2)$$

Where $P_L(d_0)$ is PL at reference distance (d_0), $(d > d_0)$, (γ) is the PLE that describes the PL variation rate as (d) increased.

With the presence of buildings and trees obstacles between TX and RX path, then log-normal fading or shadowing rise. These obstacles act as absorption causes to a part of the transmitted power affecting the (RSS) [36]. The log-normal shadowing PL model expressed as Eq. (3) [19]:

$$P_L(d) = P_L(d_0) + 10\gamma\log_{10}\left({}^{d}/_{d_0}\right) + X_\sigma \quad (3)$$

Where (X_σ) is a Gaussian random variable with zero mean and standard deviation of σ (dB). As σ gets larger, then the model is considered to be unreliable [19]. The received power $P_r(d)$ at a distance (d) and transmitted power (P_t) is shown in Eq. (4):

$$P_r(d) = P_t - P_L(d) \quad (4)$$

But since the log-distance PL model indicates that the received power decreases logarithmically as the distance (d) increases, then the average received power at distance (d) which is denoted by $(P_r(d))$ expressed as Eq. (5) [35]:

$$P_r(d) = P_r(d_0) - 10\gamma\log_{10}\left({}^{d}/_{d_0}\right) \quad (5)$$

$P_r(d_0)$, is the received power at reference distance (d_0), and it is considered the RSS Indicator (RSSI) at a certain distance (d_0) [19], and then we may get the formula in Eq. (6):

$$RSSI(d) = RSSI(d_0) - 10\gamma\log_{10}\left({}^{d}/_{d_0}\right) + X_\sigma \quad (6)$$

Where $RSSI(d)$ is RSSI at distance (d), $RSSI(d_0)$ is RSSI at reference distance (d_0) and (X_σ) equals zero at no fading.

7. Path Loss Exponent and Standard Deviation

In a wireless communication system, the PLE is a parameter that describes the rate at which the signal strength decreases with distance. Determining the PLE (γ) is crucial, as it is a

fundamental element in the design of radio signal propagation in wireless communication systems and it can predict the precision of radio propagation behavior [9]. The PLE is usually determined experimentally by measuring the RSS at different distances and fitting a model to the data. In the case of LoRaWAN, the PLE can be affected by several factors, including the operating frequency, the environment, and the type of antenna used.

One of these factors is the BW of the signal. LoRaWAN uses spread spectrum modulation, in which the data is spread over a wide frequency band. The available BW for LoRaWAN is between 125 kHz and 500 kHz. The exact value of the PLE may depend on the specific BW being used.

In general, it's expected that the PL will increase when the BW decreases. This is because a narrower BW means that the signal power is concentrated in a smaller frequency range, making it more susceptible to interference and absorption by obstacles such as buildings and trees.

It is worth mentioning that, PLE is highly dependent on the environment it's operating in. For example, in urban environments, the PLE can be higher than in rural areas due to the presence of more obstacles that can absorb or scatter the signal. Additionally, the LoRa technology is designed to work well in environments with a high PLE and a large PL, providing long-range communication.

It is also worth mentioning that, PLE is experimentally determined and can be different between various deployment scenarios or in different locations or environments.

The PLE varies depending on the specific environment and other factors such as the frequency of the signal, the type of antenna, and the presence of obstacles. Table 3 lists PLEs for different environments.

Table 3. PLEs for different environments [35]

Environment	PLE Limits
Free space	2.0
Urban	3.0 to 4.0
Suburban	2.5 to 3.5
Indoor	1.6 to 2.7
Rural	2.0 to 3.0

The PLE (γ) for one reading sample is expressed as Eq. (7):

$$\gamma = \frac{RSSI(d_0) - RSSI(d)}{10\, log_{10}\left(d/d_0\right)} 10\, log_{10}\left(d/d_0\right) \qquad (7)$$

For N reading samples (locations), (γ) is calculated by many methods, one of which is the LMS error method to reduce the error between measured $RSSI(d)$ at distance d and calculated $RSSI(d)$ using the formula in Eq. (8):

$$F(\gamma) = \sum_{i=1}^{N} (e_i)^2 = \sum_{i=1}^{N} (\text{measured RSSI} - \text{calculated RSSI})^2 \qquad (8)$$

Where e_i is the difference between measured and calculated RSSI. Equation (8) can be written as Eq. (9):

$$F(\gamma) = \sum_{i=1}^{N} \left(RSSI_i(d_i) - RSSI(d_0) - 10\gamma \log_{10}\left(d_i/d_0\right)\right)^2 \qquad (9)$$

Where ($RSSI_i$) is the measured RSSI in i-th sample at distance (d_i). The standard deviation (σ) between the measured and the calculated RSSI samples (locations) gives a good measure of the shadow fading parameter [15]. (σ) is expressed as Eq. (10):

$$\sigma = \sqrt{\frac{\sum_{i=1}^{N}(\text{measured RSSI} - \text{calculated RSSI})^2}{N}} \quad (10)$$

To get (γ), we substitute the N (N=8 samples in our case) drive test measured $RSSI_i(d_i)$ values in Eq. (9), and choosing a reference $RSSI(d_0)$ then solving the equation and differentiating it w.r.t. (γ) then equating the derivative with zero. The calculated (γ) is used to extract the PL model used to describe the environment under study.

After obtaining (γ) and (σ), Equation (6) is used to get PL model of general simplified form as in Eq. (11):

$$P_L(d) = (\alpha + \sigma) - \beta \log_{10}(d) \quad (11)$$

Where:

$$\alpha = RSSI(d_0) + \log_{10}(d_0) \quad (12)$$

$$\beta = 10\gamma \quad (13)$$

$$\sigma = \begin{cases} 0 & \text{at no shadowing effect} \\ > 0 & \text{at shadowing effect} \end{cases} \quad (14)$$

The modeling process above is explained in Fig. 4 with a flowchart.

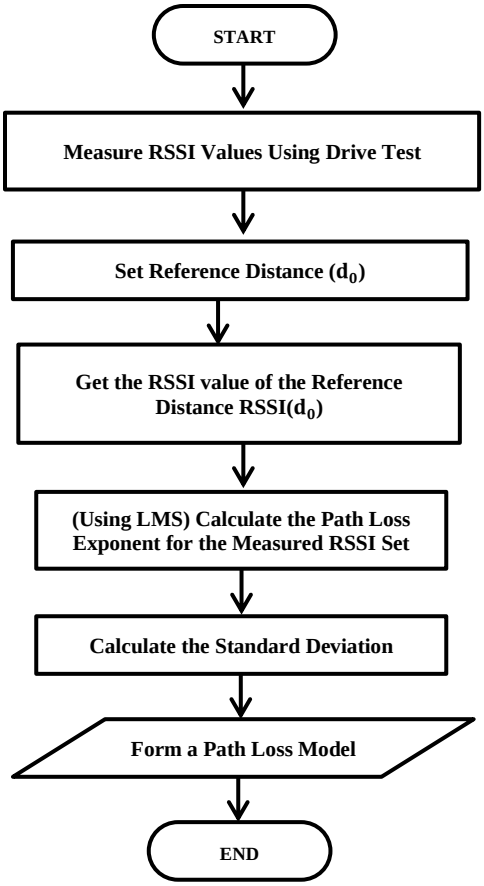

Figure 4. Modeling process flowchart

8. Results and Discussions

8.1. LoRa Performance Analysis

The overall ability of the LoRa radio RX can be determined by its RSSIs in (dBm). Table 4 summarizes the measured RSSI at eight locations with different distances from the TX in suburban sites at fixed (SF=7 and CR=4/5).

Table 4. RSSI (dBm) at fixed SF=7 and CR=4/5

BW (kHz) \ Distance (m)	20	30	50	80	100	150	215	250
125	-67	-80	-82	-93	-89	-98	-101	-99
250	-68	-76	-71	-84	-93	-95	-102	-98
500	-67	-72	-75	-89	-88	-95	-96	-93

These RSSIs are measured via drive test under V2I architecture system designed and implemented in previous work by the authors [37]. In general, LoRa parameters affect RSSI, in this work, three LoRa parameters BW, SF and CR were discussed.

As BW increased, RSSI increased (RSSI get closer to zero). Fig. 5 depicts Table 4.

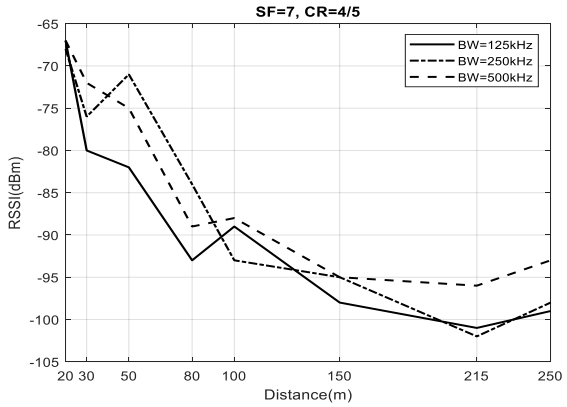

Figure 5. RSSI vs. distance at fixed SF and CR with variable BW

It can be seen that at BW=125 kHz, RSSI = -80 dBm at a distance 30 m, and for the same BW, RSSI decreases to -93 dBm at a distance 80 m, but when increasing BW to 250 kHz and then to 500 kHz, RSSIs get closer to zero for the same distance, but this is not correct in some cases due to the surrounding environment obstacles, where for BW = 250 kHz, RSSI fluctuates due to the obstacles between TX and RX.

The RSSI is also affected by the change of SF parameter, where at fixed BW = 125 kHz and CR = 4/5, RSSIs explained as shown in Fig. 6. It is seen that for distances less than 100 m, RSSI tends to be near zero, while for more than 100 m, RSSI gets farther from zero. The figure shows an overall fluctuating response of the RSSIs due to the variations of SF parameter. In general, increasing the SF will result in a lower RSSI because fewer symbols are transmitted and therefore less energy is transmitted overall. However, the exact relationship between SF and RSSI will depend on some factors, including the distance between the TX and RX, the sensitivity of the RX, and the presence of any interfering signals.

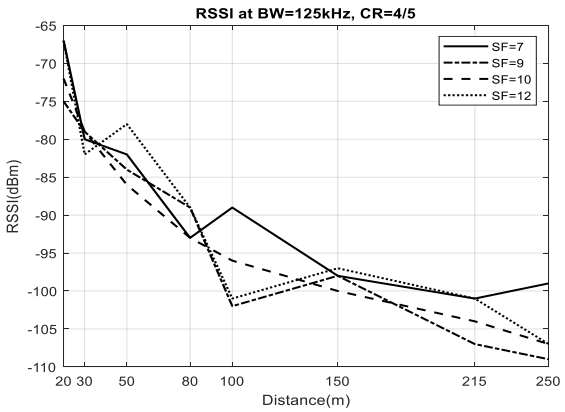

Figure 6. RSSI vs. distance at fixed BW and CR with variable SF

In general, Increase in BW may increase PL due to the reduced spreading factor and increase in noise floor, leading to a lower SNR. In LoRaWAN this is not correct most the time; there can be a number of effects on the PL. Increasing BW may reduce PL, as it allows more data to be transmitted in a given amount of time. This is because a wider BW allows for more data to be transmitted using the same amount of power, as shown in Fig. 7.

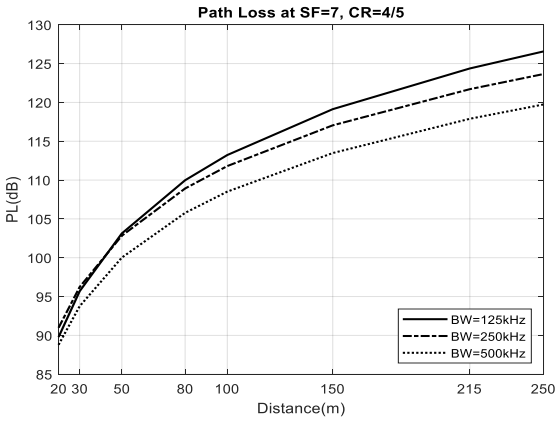

Figure 7. PL vs. distance at fixed SF and CR with variable BW

In LoRaWAN, the SF is a measure of the number of times a signal spreads over a given BW. It is one of the parameters that can be adjusted to trade-off between range and data rate in the LoRa physical layer. Increasing the SF will result in a lower data rate but a longer range because the signal spreads over a wider BW, which makes it more resistant to interference and fading. This is because the SNR is inversely proportional to the SF, so increasing the SF will decrease the SNR but also increase the range. On the other hand, decreasing the SF will result in a higher data rate but a shorter range, because the signal spreads over a narrower BW, which makes it less resistant to interference and fading, so decreasing the SF will increase the SNR but also decrease the range. Therefore, the effect of varying the SF on the PL in LoRaWAN will depend on the trade-off between the range and data rate that desired. In general, increasing the SF will result in a larger PL, but also a longer range, while decreasing the SF will result in a smaller PL, but also a shorter range, as shown in Fig. 8.

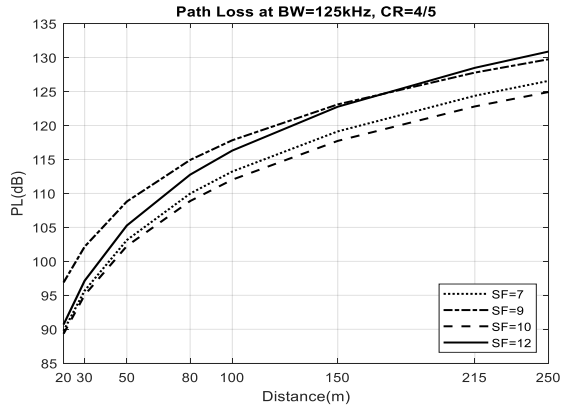

Figure 8. PL vs. distance at fixed BW and CR with variable SF

However, increasing BW can also decrease SNR due to the increased noise that is present in wider BWs. This is because the wider BW allows for more sources of interference, which can reduce the signal-to-noise ratio and increase the PL, as shown in Fig. 9(a) and Fig. 9(b).

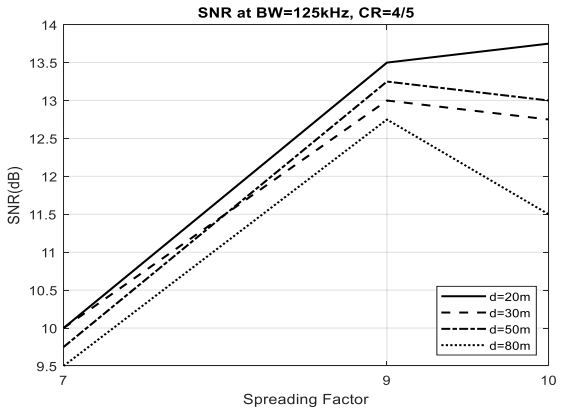

(a)

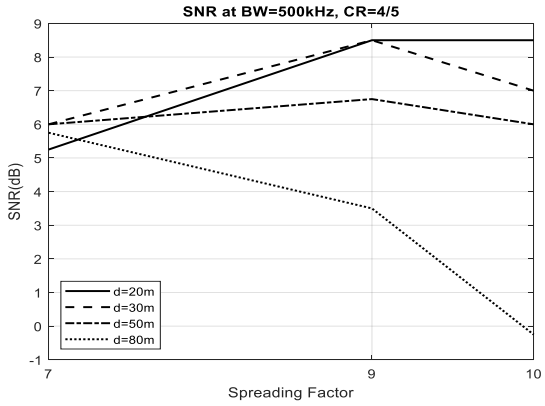

(b)

Figure 9. (a and b) SNR vs. SF at fixed CR with variable BW and distance

At (SF = 7, 9, 10, and 12 with CR=4/5) as the BW increase the PLE deviates downwards to free space behavior. While at (SF = 9) increasing BW from 250kHz to 500kHz increases PLE due to the wide frequency band with 500kHz that is affected with multiple signals between the Tx. and Rx. At (SF = 7 with CR=4/7) as BW increases the PLE downwards to free space behavior. While at (SF = 9, 10 with CR=4/7) as BW increases the PLE rises towards suburban and urban behaviors.

Changing CR from 4/5 to 4/7, the degradation of PLEs is minimized since CR offers protection against interference. So, when higher CR is provided then more protection leads to decreased PLE, as shown in Fig. 10.

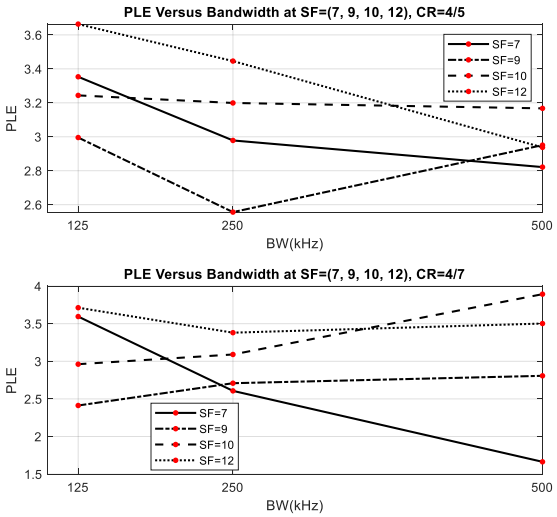

Figure 10. PLE vs. BW at variable SF and CR

Increasing BW affects the reception of data packets as SNR gets closer to the negative side (noise power greater than signal power). At BW=125 kHz, the received data rate is more than at BW=250 kHz, whereas with BW=500 kHz SNR approaches near zero dB. It can be seen that the received packets at CR=4/5 are greater than those at CR=4/7, this indicates a higher SNR at high CR, since the improvement of packet delivery ratio is obtained by increasing CR, as shown in Fig. 11.

Table 5 shows the calculated PLEs for all Semtech SX1278 LoRa module chosen configuration parameters at the drive test in this paper.

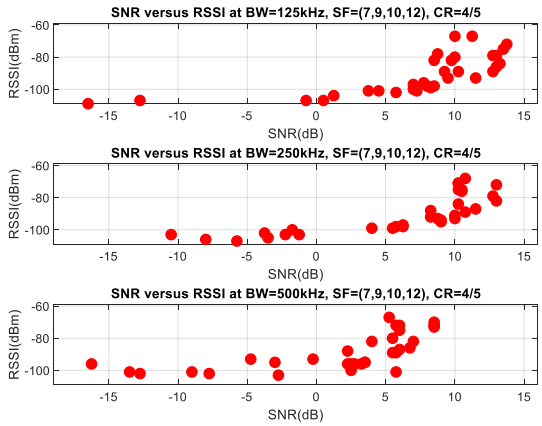

(a)

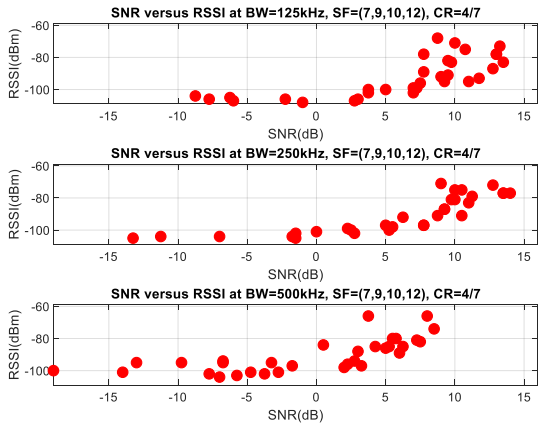

(b)

Figure 11. RSSI vs. SNR at variable SF, BW, and CR

Table 5. PLEs for chosen parameter configurations

CR	BW (kHz) \ SF	7	9	10	12
4/5	125	3.353	2.996	3.244	3.664
	250	2.978	2.556	3.199	3.446
	500	2.821	2.951	3.167	2.937
4/5	125	3.595	2.412	2.962	3.713
	250	2.607	2.709	3.091	3.380
	500	1.663	2.807	3.893	3.502

Table 6 shows the calculated standard deviations for all Semtech SX1278 LoRa module chosen configuration parameters at the drive test.

Table 6. Standard deviations for chosen parameter configurations

CR	BW (kHz) \ SF	7	9	10	12
4/5	125	5.786	4.889	0.346	6.699
	250	5.985	3.105	5.906	7.337
	500	4.791	4.785	6.585	5.405
4/5	125	6.748	5.861	1.829	4.330
	250	4.717	5.982	4.952	4.664
	500	5.303	4.219	8.431	7.153

8.2. Path Loss Optimization

Once the PL is mathematically calculated, the minimization of PL can be characterized. The objective is to find the policy (AP_L) that minimizes the accumulated PL. The policy is defined by the set {SF, BW, CR}, that is, the configuration combinations employed to LoRa module when transmitting.

Equation (15) formally defines this minimization of (AP_L):

$$\text{minimize } AP_L\{SF, BW, CR\} = \sum_{i=1}^{8} P_L(d_i).\omega_i \quad (15)$$

Table 7 briefs the symbols in Eq. (15):

The set configuration {SF, BW, CR} has possible 24 combinations which return different values of drive test measured RSSIs, these lead to different calculated values of PLs for each {SF, BW, CR} combination at each distance under consideration.

Table 7. Minimization policy symbols

Symbol	Representation
AP_L	Accumulative PL value at i distance in meters, $i = 20, 30, 50, 80, 100, 150, 215\ and\ 250$
ω	weighting vector, $\omega = 0.05, 0.05, 0.1, 0.1, 0.15, 0.15, 0.2, 0.2$
SF	the selected SF values, $SF = [7, 9, 10, 12]$
BW	the selected BW values in kHz, $BW = [125, 250, 500]$
CR	the selected CR values, $CR = [4/5, 4/7]$

The goal is to find the minimum PL according to the above policy. Fig. 12 depicts the optimal PL at {SF, BW, CR} set for different distances.

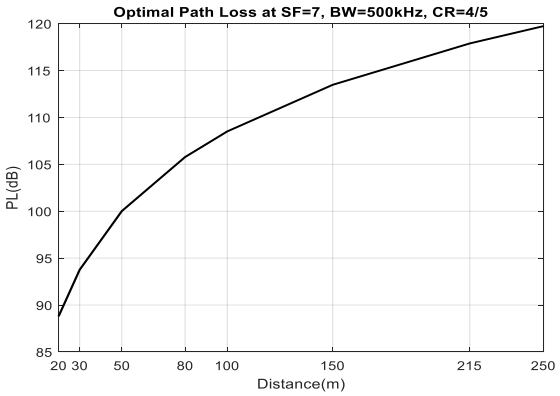

Figure 12. Optimal PL

9. Conclusions and Future Works

In this paper, a generalized PL model presented for suburban environments, based on empirical propagation modeling and real-world drive test RSSI measurements. The design of a LoRaWAN-based IoV system was analyzed in terms of PL measurements. The impact of LoRa parameters, including SF, BW, and CR on link performance was evaluated by estimating coverage range and PL using the PLE calculation. The results indicated that tuning BW affects RSSI to be fluctuating due to obstacles between TX and RX. Increasing BW may decrease PL and SNR. Also, tuning SF affects RSSI to fluctuate w.r.t distance, RX sensitivity, and obstacles. Increasing SF results in larger PL. The results indicated that the PLE is subject to instability due to variations in the LoRa parameters. The relationship between received packet rate, RSSI, and SNR was also analyzed for different LoRa parameters. An optimal policy was proposed to minimize PL, and the results indicated that based on the measured RSSIs and predicted PL model, the optimal PL was achieved using the LoRaWAN parameters of SF = 7, BW = 500 kHz, and CR = 5.

In the future, this work may be developed through the consideration of different antenna heights and analyzing its effect on the link performance of such PL modeling then comparing it with other propagation PL models such as Okumura-Hata model. Also, other sites may be considered in this study, such as urban sites. Furthermore, the effect of vehicle speed may be considered for future analysis.

Acknowledgments

The authors would like to thank Mustansiriyah University (www.uomustansiriyah.edu.iq) Baghdad – Iraq for its support in the present work.

Conflict of interest

The authors confirm that there is no conflict of interest associated with the publication of this article.

Author Contribution Statement

The manuscript was written and edited by all authors. The research problem was initiated by Gregor A. Aramice; with supervision from Dr. Abbas H. Miry and Dr. Tariq M. Salman. The introduction and manuscript style were developed by all authors and the results were discussed and incorporated into the final version by all authors.

References

1. Wortmann, F., Flüchter, K. (2015). *Internet of Things: technology and value added*. Business & Information Systems Engineering, Springer. Vol. 57, Issue: 3, pp. 221–224. https://doi.org/10.1007/s12599-015-0383-3

2. Karim, S. M., Habbal, A., Chaudhry, S.A., and Irshad, A. (2022). *Architecture, Protocols, and Security in IoV: Taxonomy, Analysis, Challenges, and Solution*. Security and Communication Networks. Vol. 2022. https://doi.org/10.1155/2022/1131479

3. Álamos, A., Kietzmann, P., Schmidt, T. and Wählisch, M. (2022). *DSME-LoRa: Seamless Long-range Communication between Arbitrary Nodes in the Constrained IoT*. ACM Transactions on Sensor Networks. Vol. 18, Issue 4, pp. 1-43. https://doi.org/10.1145/3552432

4. Haxhibeqiri, J., Karaagac, A., Abeele, F.V., Joseph, W., Moerman, I., Hoebeke, J. (2017). "*LoRa indoor coverage and performance in an industrial environment: Case study*". Proc. of the 22nd IEEE Int. Conf. on Emerging Technologies and Factory Automation, Cyprus, pp. 1-8. https://doi.org/10.1109/ETFA.2017.8247601

5. Avila-Campos, P., Astudillo-Salinas, F., Vazquez-Rodas, A. and Araujo, A. (2019). "*Evaluation of LoRaWAN Transmission Range for Wireless Sensor Networks in Riparian Forests*". Proc. of the 22nd Int. ACM Conf. on Modeling, Analysis and Simulation of Wireless and Mobile Systems (MSWIM '19). Association for Computing Machinery, New York, NY, USA, pp. 199–206. https://doi.org/10.1145/3345768.3355934

6. Harvanova, V. and Krajcovic, T. (2011). "*Implementing ZigBee network in forest regions - Considerations, modeling and evaluations*". Int. Conf. on Applied Electronics, Czech Republic, pp. 1–4.

7. Kongsavat, A., and Karupongsiri, C. (2020). "*Path Loss Model for Smart Meter on LoRaWAN Technology with Unidirectional Antenna in an Urban Area of Thailand*". IEEE Int. Conf. on Computational Electromagnetics (ICCEM), Singapore, pp. 260-262. https://doi.org/10.1109/ICCEM47450.2020.9219522

8. Nsaif, B.G., and Sallomi, A.H. (2021). *Path Loss Modeling For Urban Wirless Networks In Baghdad*. Journal of Engineering and Sustainable Development (JEASD). Vol. 25, Issue: Special_ Issue_2021, pp. 1-7-1-12. https://doi.org/10.31272/jeasd.conf.2.1.2

9. Rademacher, M., Linka, H., Horstmann, T., and Henze, M. (2021). "*Path Loss in Urban LoRa Networks: A Large-Scale Measurement Study*". *IEEE 94th Vehicular Technology Conf. (VTC2021-Fall)*, Norman, OK, USA, pp. 1-6. https://doi.org/10.1109/VTC2021-Fall52928.2021.9625531

10. Karttunen, A., Gustafson, C., Molisch, A.F., Wang, R., Hur, S., Zhang, J., Park, J. (2016). *Path loss models with distance-dependent weighted fitting and estimation of censored path loss data*. IET Microwave Antennas Propagation. Vol. 10, Issue: 14, pp. 1467-1474. https://doi.org/10.1049/iet-map.2016.0042

11. Allen, B., Mahato, S., Gao, Y., and Salous S. (2017). *Indoor-to-outdoor empirical path loss modelling for femtocell networks at 0.9, 2, 2.5 and 3.5 GHz using singular value decomposition*. IET Microwave Antennas Propagation, Vol. 11, Issue: 9, pp. 1203-1211. https://doi.org/10.1049/iet-map.2016.0416

12. Unterhuber, P., Sand, S., Fiebig, U.C., and Siebler B. (2018). *Path loss models for train-to-train communications in typical high speed railway environments*. IET Microwave Antennas Propagation, Vol. 12, Issue: 4, pp. 492-500. https://doi.org/10.1049/iet-map.2017.0600
13. Bertoldo, S., Paredes, M., Carosso, L., Allegretti, M. and Savi, P. (2019). "*Empirical indoor propagation models for LoRa radio link in an office environment*". IEEE 13th European Conf. on Antennas and Propagation (EuCAP), Krakow, Poland, pp. 1-5.
14. Ingabire, W., Larijani, H., and Gibson, R.M. (2020). "*Performance Evaluation of Propagation Models for LoRaWAN in an Urban Environment*". IEEE International Conference on Electrical, Communication, and Computer Engineering (ICECCE), Istanbul, Turkey, pp. 1-6. https://doi.org/10.1109/ICECCE49384.2020.9179234
15. Zakaria, Y.A., Hamad, E.K.I., Elhamid, A.S.A. and El-khatib, K.M. (2021). *Developed channel propagation models and path loss measurements for wireless communication systems using regression analysis techniques*. Bulletin of the National Research Centre, Vol. 45, Issue: 54. https://doi.org/10.1186/s42269-021-00509-x
16. Gaboitaolelwe, J., Zungeru, A.M., Chuma, J., Ditshego, N. and Semong, T. (2020). *A Formal Analytical Modeling and Simulation of Wireless Sensor Home Network*. International Journal of Intelligent Engineering and Systems. Vol. 13, Issue: 3, pp. 56-68. http://repository.biust.ac.bw/handle/123456789/390
17. Wu, H., Zhang, L., and Miao, Y. (2017). *The Propagation Characteristics of Radio Frequency Signals for Wireless Sensor Networks in Large-Scale Farmland*. Wireless Personal Communication, Vol. 95, pp. 3653–3670. https://doi.org/10.1007/s11277-017-4018-5
18. Callebaut, G. and Perre, L.V. (2019). *Characterization of LoRa Point-to-Point Path Loss: Measurement Campaigns and Modeling Considering Censored Data*. IEEE Internet of Things Journal. Vol. 7, Issue: 3, pp. 1910-1918. https://doi.org/10.1109/JIOT.2019.2953804
19. Lin, Y., Dong, W., Gao, Y., and Gu, T. (2020). "*SateLoc: A Virtual Fingerprinting Approach to Outdoor LoRa Localization using Satellite Images*". 19th ACM/IEEE International Conference on Information Processing in Sensor Networks (IPSN), Sydney, NSW, Australia, pp. 13-24. https://doi.org/10.1145/3461012
20. Lin, K. and Hao, T. (2021). *Experimental Link Quality Analysis for LoRa-Based Wireless Underground Sensor Networks*. IEEE Internet of Things Journal. Vol. 8, Issue: 8, pp. 6565-6577. https://doi.org/10.1109/JIOT.2020.3044647
21. Akram, S.V., Singh, R., AlZain, M.A., Gehlot, A., Rashid, M., Faragallah, O.S., El-Shafai, W. and Prashar, D. (2021). *Performance Analysis of IoT and Long-Range Radio-Based Sensor Node and Gateway Architecture for Solid Waste Management*. Sensors, Vol. (21), Issue: 8. https://doi.org/10.3390/s21082774
22. Anzum, R., Habaebi, M.H., Islam, M.R., Hakim, G.P.N., Khandaker, M.U., Osman, H., Alamri, S. and AbdElrahim, E. (2022). *A Multiwall Path-Loss Prediction Model Using 433 MHz LoRa-WAN Frequency to Characterize Foliage's Influence in a*

Malaysian Palm Oil Plantation Environment. Sensors (Basel). Vol. 22, Issue: 14. https://doi.org/10.3390/s22145397

23. Budi, A. H. S., Juanda, E. A., Kustiawan, I., Kurniadi, N. N. N. and Henny, H. (2021). *River Water Monitoring System Using Internet Of Things To Determine The Location Of River Pollution*. Journal of Engineering Science and Technology, Vol. 16, Issue: 4, pp. 3222-3233.
24. Staniec, K., and Kowal, M. (2018). *LoRa Performance under Variable Interference and Heavy-Multipath Conditions*. Wireless Communications and Mobile Computing, Hindawi. https://doi.org/10.1155/2018/6931083
25. Bor, M.C., Roedig, U., Voigt, T. and Alonso, J.M. (2016). "*Do LoRa Low-Power Wide-Area Networks Scale?*". Proc. of the 19th ACM Int. Conf. on Modeling, Analysis and Simulation of Wireless and Mobile Systems (MSWiM '16), Association for Computing Machinery, New York, NY, USA, pp. 59–67. https://doi.org/10.1145/2988287.2989163
26. Saari, M., Baharudin, A. M., Sillberg, P., Hyrynsalmi, S. and Yan, W. (2018). "*LoRa — A survey of recent research trends*". 41st International Convention on Information and Communication Technology, Electronics and Microelectronics (MIPRO), Opatija, Croatia, pp. 0872-0877. https://doi.org/10.23919/MIPRO.2018.8400161
27. Ertürk, M.A., Aydın, M.A., Büyükakkaşlar, M.T. and Evirgen, H. (2019). *A Survey on LoRaWAN Architecture, Protocol and Technologies*. Future Internet, Vol. 11, Issue: 10. https://doi.org/10.3390/fi11100216
28. https://www.semtech.com/products/wireless-rf/lora-connect/sx1278
29. Janczak, D., Walendziuk, W., Sadowski, M., Zankiewicz, A., Konopko, K. and Idzkowski, A. (2022). *Accuracy Analysis of the Indoor Location System Based on Bluetooth Low-Energy RSSI Measurements*. Energies. Vol. 15, Issue: 23. https://doi.org/10.3390/en15238832
30. Coleman, D. D. and Westcott, D. A. (2018). *CWNA: Certified Wireless Network Administrator Study Guide: Exam CWNA-10X*. 5th ed. 2018, Canada: John Wiley & Sons, Inc. ISBN: 9781119549406.
31. Bor, M., Vidler, J. and Roedig, U. (2016). "*LoRa for the Internet of Things*". Proc. of the 2016 Int. Conf. on Embedded Wireless Systems and Networks (EWSN '16). Junction Publishing, USA, pp. 361–366. https://eprints.lancs.ac.uk/id/eprint/77615
32. Kaiwartya, O., Abdullah, A., Cao, Y., Altameem, A., Prasad, M., Lin, C. and Liu, X. (2016). *Internet of vehicles: motivation, layered architecture, network model, challenges, and future aspects*. IEEE Access, Vol. 4, pp. 5356-5373. https://doi.org/10.1109/ACCESS.2016.2603219
33. Oestges, C. and Quitin, F. (2021). *Inclusive Radio Communications for 5G and Beyond*. 1st ed. Academic Press. ISBN: 9780128205815
34. Seybold, J.S. (2005). *Introduction to RF Propagation*. John Wiley & Sons. ISBN: 978-0-471-65596-1.
35. Rappaport, T.S. (2002). *Wireless Communications: Principles and Practice*. 2nd ed. Prentice Hall Press.
36. Shang, F., Su, W., Wang, Q., Gao, H. and Fu, Q. (2014). *A Location Estimation Algorithm Based on RSSI Vector Similarity Degree*. International Journal of Distributed Sensor Networks. Vol. 10, Issue: 8, pp. 1–22. http://dx.doi.org/10.1155/2014/371350

37. Aremice, G.A, Miry, A.H. and Salman, T.M (2023). *Vehicle Black Box Implementation For Internet Of Vehicles Based Long Range Technology*. Journal of Engineering and Sustainable Development (JEASD). Vol. 27, Issue: 2, pp. 245-255. https://doi.org/10.31272/jeasd.27.2.8